**ACTA IMEKO**
**ISSN: 2221-870X**
*June 2022, Volume 11, Number 2, 1 - 7*

# A strategy to control industrial plants in the spirit of Industry 4.0 tested on a fluidic system

**Laura Fabbiano[1], Paolo Oresta[1], Rosario Morello[2], Gaetano Vacca[1]**

[1] *DMMM, Politecnico di Bari University, Bari, Italy*
[2] *DIIES, University Mediterranea of Reggio Calabria, Italy*

ABSTRACT
The goal of the paper is to propose a strategy of automating the control of wide spectrum industrial processes plants in the spirit of Industry 4.0. The strategy is based on the creation of a virtual simulator of the operation of the plants involved in the process. Through the digitization of the operational data sheets of the various components, the simulator can provide the reference values of the process control parameters to be compared with their actual values, to decide the direct inspection and/or the operational intervention on critical components before a possible failure. As example, a simple fluidic thrust plant has been considered, which a mathematical model (simulator) for its optimal operating conditions has been formulated for, by using the digitalized real operational data sheets of its components. The simple thrust system considered consists of a centrifugal pump driven by a three-phase electric motor, an inverter to regulate the rotation of the motor and a proportional valve that simulates the external load acting on the pump.
As results, the operational data sheets and principal characteristics of the pump have been reproduced by means of the simulator here developed, showing a very good agreement.

**Section:** RESEARCH PAPER

**Keywords:** Industry 4.0; predictive maintenance; prognostic approach; plant operation simulator; fluidic thrust plant

**Citation:** Laura Fabbiano, Paolo Oresta, Rosario Morello, Gaetano Vacca, A strategy to control industrial plants in the spirit of Industry 4.0 tested with fluidic devices, Acta IMEKO, vol. 11, no. 2, article 31, June 2022, identifier: IMEKO-ACTA-11 (2022)-02-31

**Section Editor:** Francesco Lamonaca, University of Calabria, Italy

**Received** November 9, 2021; **In final form** February 21, 2022; **Published** June 2022



**Corresponding author:** Laura Fabbiano, e-mail: laura.fabbiano@poliba.it

## 1. INTRODUCTION

The costs of maintenance are a consistent amount of the total operating costs in industrial production. Moreover, several extra costs come from the profit loss due to the undesired failure of the plant. They can be dropped down with a failure prediction that preserves the devices through just on-time maintenance.

These two classes of problems can be solved by the implementation of preventive maintenance in the perspective of the smart industry, [1]-[3], for which all the elements of a factory work in a completely, collaborative and integrated way and deal in real-time with the timely changes of the workflow.

Concerning costs reduction in force of the just on-time failure detection, the goal of the smart industry is to implement all the fundamental measurement procedures for continuous real-time monitoring (real-time condition monitoring) and coordinated monitoring of all plant elements, [4]-[6].

The keywords of the fourth industrial revolution are, therefore "preventive maintenance", "intelligent and real-time orchestration" and "synchronization of physical and digital processes".

In literature, there are crucial new insights about the continuous screening of the devices that made possible the detection of incipient failure, [7]-[9]. Among others, the prognostic approach is mandatory to obtain an accurate and coding of incipient machine failures, [10]-[12]. The detection of the degradation and damage of a plant component is the goal of the predictive approach. The condition-based maintenance (CBM) specifications [13], [14] inspired by the prognostic approach has been applied by the authors to the case of a simple fluidic thrust system by using a mathematical approach. It consists of a pump-motor block with inverter and a control valve, which represents the load acting on the P-M block and attributable to the network supplied by it.

The approach uses a numerical simulator to manage and analyse in real-time all the characteristic parameters (sensed or mathematically predicted) of each system components to get and to advise concerning likely incipient anomalies of the monitored components.

The virtual simulator is based on the digital reconstruction of the data sheets of all the more sensitive components of the system to allow the digital prediction of the optimal point of system working conditions. These data provided by model are compared with the real-time instantaneous acquisitions of the correspondent main operating parameters. The eventual discrepancy between virtual and actual values of the monitored parameter identifies which of the components of the system may be in critical conditions, thus dropping down its start and stop time responsible of the maintenance and service interruption costs. The proposed procedure, based on the digitization of the technical data sheets of the plant devices can be easily extended to most of the systems operating in industrial processes, thus allowing to control the entire system in real-time and detecting the dangerous failure scenarios.

## 2. PLANT SPECIFICATIONS

The system here simulated is a simple fluidic thrust plant and consists of a centrifugal pump (CALPEDA NM4 25/12A/A, [15]) driven by an electric asynchronous motor whose rotation speed is regulated by an inverter, and a control valve simulating the supplied network. The operational point of such system is determined by the coupling of the pump with the valve. The technical and geometric characteristics of each component are known. Those of the pump are here reported:

| | |
|---|---|
| $n = 1450$ rpm | rotational speed of reference |
| $P = 0.25$ kW | absorbed power at 1450 rpm |
| $Q = 1 \div 6$ m$^3$/h | flow rate working range |
| $H_u = 6.1 \div 3.3$ m | head range |
| $D_2 = 131.5$ mm | external diameter of the impeller |
| $\beta_2 = 157.5°$ | angle of blade exit |
| $l_2 = 4$ mm | blade height |
| $z = 7$ | number of blades |
| $\zeta = 1 - \frac{zs}{\pi D_2} = 0.95$ | blade bulk coefficient |

A user interface has been set up to manage the procedure of analysis and acquisition of data. Specifically, that interface has been created on LabVIEW platform and is divided into several sections; each section manages and analyses the different parts of the plant, Figure 1.

In the control section you find the commands to change the opening degree of the valve and the inverter frequency.

The target section enforces the rotation number of the engine. Once the frequency is set by the control panel, it automatically varies until the system reaches a stable point of operation where the number of revolutions of the pump coincides with the value imposed in the target panel.

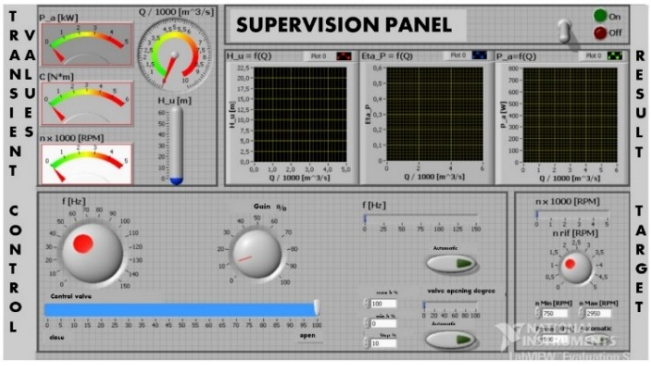


Figure 1. User interface in LabVIEW platform.

The transient panel shows the indicators of instant monitoring of the plant. In particular, the quantities acquired by the transducers (number of revolutions, mechanical torque, flow rate, head) and some derived quantities such as instantaneous absorbed power are represented.

The results panel collects in graphic form (three different plots) the trends of the pump head (characteristic curve), efficiency and absorbed power as a function of the flow rate.

## 3. VIRTUAL SIMULATOR

The mathematical model of the plant consists of:

1. valve model;
2. pump - motor block model.

Most of the geometric and operating data have been inferred from the technical specifications of the components.

### 3.1. Valve model

The control valve (here a proportional solenoid valve) allows the modulation of the circuit external characteristic (valve characteristic), [16]. That is, by acting on the closing/opening control devise, the relationship between the pressure drops and the flow rate flowing through the valve changes, so determining a new operating point as intersection with the internal characteristic (pump operating curve).

From Bernoulli's equation the relationship to the basis of the valve operation comes out as:

$$Q = \left[c_{v_{\max}} h + c_{v_{\min}}(1-h)\right]\sqrt{\frac{H_v}{H_v^*}}, \tag{1}$$

where:

- $0 < h < 1$ degree of opening of the valve (or shutter stroke);
- $c_{v_{\max}} = 0.005$ m$^3$/h and $c_{v_{\min}} = 10^{-6}$ m$^3$/h flow rates (or efflux coefficients) minimum and maximum estimated by the technical data sheet of the pump;
- $H_v \rightarrow$ static pressure drop through the valve (m);
- $H_v^* \rightarrow 1\ psi$ static pressure drop through the valve (m). It represents the linear operational limit of the valve itself.

From the previous relationship we get:

$$H_v = Q^2 \frac{H_v^*}{\left[c_{v_{\max}} h + c_{v_{\min}}(1-h)\right]^2} \tag{2}$$

If a linear valve is considered, its characteristic coefficient $K_v(h)$ reads as:

$$K_v(h) = \frac{H_u^*}{\left[c_{v_{max}} h + c_{v_{min}}(1-h)\right]^2}, \tag{3}$$

so, making possible to rewrite the previous relation as:

$$H_v = Q^2 K_v(h) \tag{4}$$

The efflux coefficient of the valve is an increasing monotonous function of the shutter stroke, $c_v(h)$, and it can be expressed in dimensionless form if the following quantities are considered:

- the relative efflux coefficient: $\varphi = c_v / c_{\max}$
- the intrinsic rangeability, ratio between the maximum and the minimum values of the efflux coefficient: $r = c_{v_{\max}} / c_{v_{\min}}$

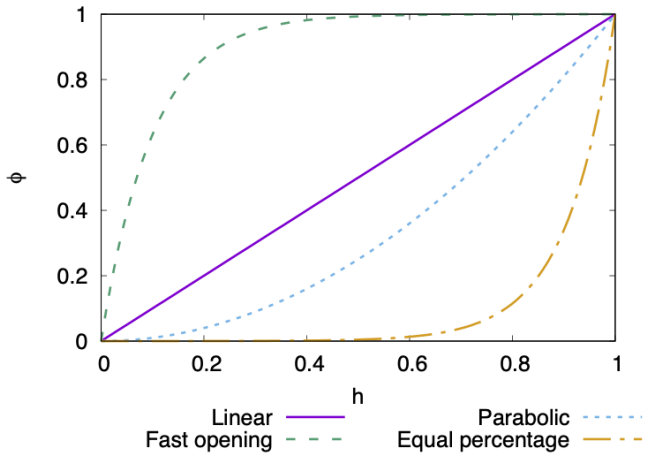


Figure 2. Valve characteristic curves in terms of the flow rate coefficient, $\phi$ as function of the opening position, $h$. The curves show the cases of linear, parabolic, equal percentage and fast opening design.

Examples of valve characteristics expressed in terms of $h$ are shown in Figure 2 for linear, equal percentage, fast-opening and quadratic valves:

For the linear characteristic, it holds the relation:

$$\varphi(h) = h + \frac{1}{r}(1-h) \tag{5}$$

In the plant operating model (simulator), the characteristic coefficient of the valve can be rewritten as, from (4):

$$K_v(h) = \frac{H_v^*}{c_v(h)^2} = \frac{H_v^*}{c_{v\max}^2 \varphi(h)^2} \tag{6}$$

this relation for $K_v(h)$ keeps holding even for other kind of valves, if the right formula for $\varphi(h)$ is introduced in it.

### 3.2. Motor pump block

The 'Pump-Motor' block, Figure 3, represents the virtual simulator of a centrifugal pump and its electric control motor.

This block has 2 inputs and 4 outputs. The 2 inputs are, respectively:

1. The coefficient of the valve, whose operating characteristic is enclosed in the *'Valve'* model and is provided by it. Its regulation will result in the variation of the number of revolutions of the pump, $n$
2. The magnetic field frequency, parameter recalled by the control unit, which allows to act in feedback on it, in order to restore the number of revolutions to a target and constant value during the process of digital reconstruction of the characteristic curves of the pump.

The 4 outputs represent the virtual sensors of the P-M block suitable for the detection of:

1. Q flow rate (m³/h)
2. $H_u$ head provided by the pump (m)
3. $n$ number of engine revolutions (rpm)
4. $C_m$ drive torque, (N m).

They are recalled by the supervisor function (see Figure 1) and made visible in the transient panel, where the instant monitoring indicators of the system are reported. In particular, the quantities


Figure 3. Inputs and outputs of the pump-motor block.

Table 1. Pump data.

| Q in m³/h | 1 | 1.2 | 1.5 | 1.8 | 2.4 | 3 | 3.6 | 4.2 | 4.8 | 5.4 | 6 |
|---|---|---|---|---|---|---|---|---|---|---|---|
| H in m | 6 | 6.05 | 6 | 5.9 | 5.8 | 5.5 | 5.2 | 4.8 | 4.4 | 3.9 | 3.3 |

acquired by the transducers (for a number of revolutions, mechanical torque, flow rate, head) and some derived quantities such as the instantaneous absorbed power are shown.

In the model there are some geometric parameters directly available from the technical characteristics of the pump; other necessary parameters are inferred from the characteristic curves and the power absorbed by the pump, for a fixed pump revolution.

The internal characteristic of the pump at the revolution $n_0 = 450$ rpm can be expressed in polynomial form as follows:

$$H_u = -0.0893\, Q^2 + 0.0706\, Q + 6.104 \tag{7}$$

obtained by best square polynomial regression of the pump, reported in the Table 1 and shown in Figure 4.

It is possible to generalize this relation and make it valid for any number of revolutions, as:

$$H_u = a\, Q^2 + b\frac{n}{n_0} Q + c\left(\frac{n}{n_0}\right)^2 \tag{8}$$

where $a, b$ and $c$ are the coefficients of the specific previous relation.

Substituting the expression of the valve characteristic (4) in (8), in the steady state operating condition of the system, we obtain:

$$[a - K_v(h)]Q^2 + b\frac{n}{n_0} Q + c\left(\frac{n}{n_0}\right)^2 = 0. \tag{9}$$

By expressing then $Q$ as a function of the geometrical and operating parameters of the pump as:

$$Q = K_Q\, \varphi\, n\,, \tag{10}$$

where $K_Q = \eta_v\, \zeta\, \pi^2\, l_2\, D_2^2$, and substituting it in the equation that regulates the operation of the plant (9) we get the new relation:

$$K_{\phi_0}^2 [a - K_v(h)]\phi^2 + bK_{\phi_1}\phi + K_{\phi_2} = 0\,, \tag{11}$$

where $K_{\phi_0} = K_Q^2\, n_0^2 [a - K_v(h)]$, $K_{\phi_1} = b\, K_Q\, n_0$, $K_{\phi_2} = c$, and $\phi$ the flow parameter.

The equality of the head provided by the pump with the pressure drop introduced by the control valve is not sufficient to describe the operation of the experimental system. We need the

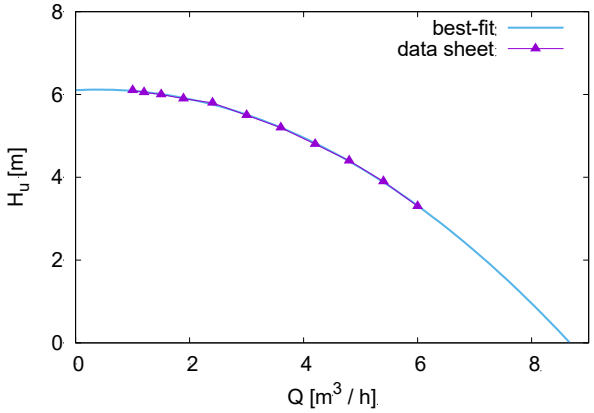


Figure 4. Pump performance curve at $n = 1450$ rpm. Comparison between simulation and actual operational point.

power conservation law, for which the power supplied by the motor equals the power absorbed by the pump.

The last one is expressed by:

$$P_{a_p} = \frac{\gamma\, Q\, H_u}{\eta_y\, \eta_v\, \eta_m} = \frac{\rho\, Q\, L_i}{\eta_v\, \eta_m} = \frac{\rho\, K_Q\, \phi\, \psi\, \pi\, D^2\, n^2}{2\, \eta_v\, \eta_m} \tag{12}$$

in which $\psi = 2(1 - \phi\, \mathrm{cotg}\beta_2) - (2\, \pi \sin \beta_2)/z$ and $\eta_v$ *ed* $\eta_m$ are the volumetric and mechanical efficiencies to be discussed in the paragraph of the results, where the methods to evaluate their values during the actual operation of the plant for its monitoring will be described. Both could result indices of possible anomalies.

With reference to the expression of the power supplied by the motor, $P_m$, the mechanical torque, $C_m$, can be expressed.

The mechanical torque $C_m$ of the electric motor can be expressed as a function of the slip, $s$, according to the following relation:

$$C_m = 2C_{m_{\max}} \frac{s_{\max} \cdot s}{(s_{\max}^2 + s^2)} \tag{13}$$

in which $C_{m_{\max}}$ is the maximum torque available for the slip value $s = s_{\max}$, available from the relative data sheet and equal to $C_m = 50$ N m and $s = 0.2$.

The slip is representative of the difference between the speed of rotation of the rotor, i.e., the shaft and the speed of rotation of the magnetic field, $n_s$,that is:

$$s = \frac{n_s - n}{n_s}, \tag{14}$$

where:

$$n = \frac{60f}{p}\,(1 - s) \tag{15}$$

with $p = 2$, motor polar couples.

The mechanical characteristic of the motor, $C_m$, is represented as function of the revolution of the shaft in Figure 5 for 3 different values of frequency.

This characteristic shows that when the slip is roughly zero the torque reaches its maximum value, and the motor speed is close to the synchronism speed $n_s$.

The efficiency $\eta$ of the three-phase asynchronous motor can be calculated with the well-known formula:

$$\eta = \frac{P_r}{P_a}, \tag{16}$$

where $P_r$ is the mechanical power supplied to the rotor and $P_a$ is the electrical power provided by the stator.

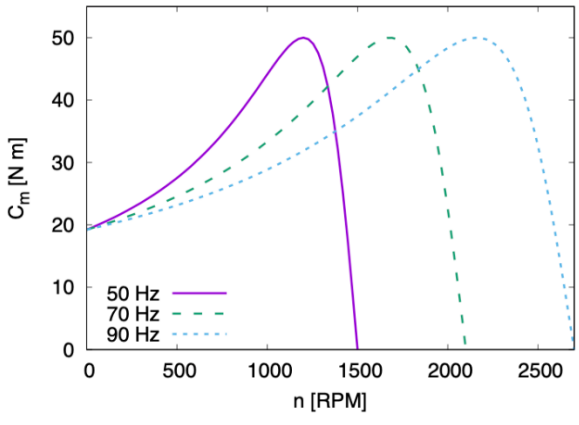


Figure 5. Characteristics of the asynchronous motor in terms of torque as function of revolution, for different frequency values.

Equating the power absorbed by the pump to the power supplied by the motor, we obtain:

$$\frac{\rho\, K_Q\, \phi\, \psi\, \pi\, D^2\, n^2}{2\, \eta_v\, \eta_m} = \left(2C_{m_{\max}} \frac{s_{\max} \cdot s}{{s_{\max}}^2 + s^2}\right) 2\, \pi\, n \tag{17}$$

and plugging into it the expression of the slip $s$, we get:

$$\begin{aligned} &\rho\, K_Q\, \phi\, \psi\, \pi\, D_2^2 \left(\frac{p}{f}\right)^2 n^4 - \frac{\rho\, K_Q\, \phi\, \psi\, \pi\, D_2^2\, 2\, p}{f} n^3 \\ &+ \rho\, K_Q\, \phi\, \psi\, \pi\, D_2^2 (s_{\max} + 1)\, n^2 \\ &+ 8\, C_{m_{\max}}\, s_{\max}\, \eta_v\, \eta_m \frac{p}{f} n \\ &- 8\, C_{m_{\max}}\, s_{\max}\, \eta_v\, \eta_m = 0. \end{aligned} \tag{18}$$

The previous equation can be rewritten in the easier-to-read following way:

$$K_{n0}\, n^4 + K_{n1}\, n^3 + K_{n2}\, n^2 + K\, n_3\, n + K_{n4} = 0, \tag{19}$$

with obvious meaning of the symbols.

The former equation represents the main equation of the plant operating model. Such an equation can be solved iteratively by the Newton-Raphson method, for example, to provide the revolution speed of the system for a fixed working condition. The iterations, in the present case, have been interrupted when the percentage error on $n$ was less than $10^{-5}$.

The described set of model equations of the thrust system components constitute the simulator of its working operation.

## 4. RESULTS

The volumetric efficiency of the pump changes according to the operating regime. It is negligible for null flow rates in the case of a control valve fully closed. As the flow rate increases, the volumetric efficiency increases up to the plateau value that is almost constant for a wide range of the pump flow rate, in steady state operation. The data sheet values of it are shown in Figure 6 here below.

In the case of high flow rate, the following procedure aims to calculate the values of the mechanical and the volumetric efficiencies, $\eta_m$, $\eta_{v\infty}$ (asymptotic value), respectively. The pressure parameter, $\psi$, can be computed, in the following two ways:

$$\psi = \frac{2\, g\, H_u}{u_2^2\, \eta_p} \eta_m \eta_y \tag{20}$$

or

$$\psi = 2(1 + \phi\, \mathrm{cotg}\, \beta_2) - \frac{2\, \pi \sin \beta_2}{z}. \tag{21}$$

Equating the above equations and rewriting the flow parameter as a function of the flow rate, $\phi = \phi(Q)$, we get:

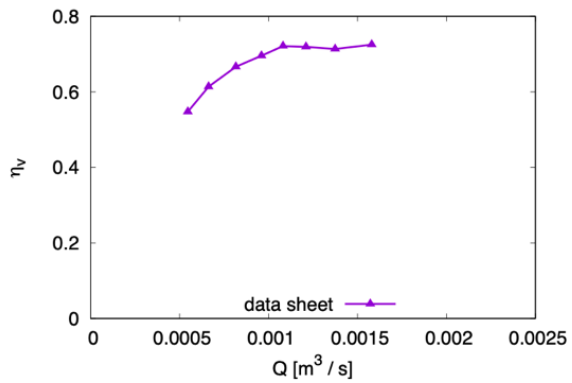


Figure 6. Pump volumetric efficiency experimental data.

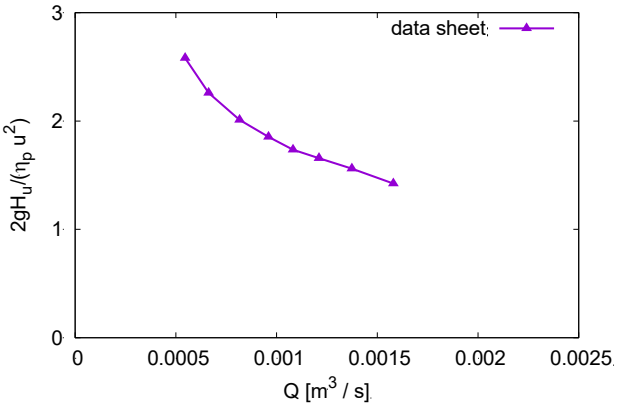


Figure 7. experimental values for the left-hand side term in (22) as a function of the flow rate.

$$\frac{2\,g\,H_u}{u_2^2\,\eta_p} = \frac{2\,\mathrm{cotg}\,\beta_2}{\eta_v\,\xi\,\pi^2\,l_2\,D_2^2\,n}\,\frac{1}{\eta_m\,\eta_v}\,Q + \frac{2}{\eta_m\,\eta_v}\left(1-\frac{\pi\sin\beta_2}{z}\right). \tag{22}$$

From the experimental data of the pump CALPEDA NM4 25/12A/A, it is observed that for flow rates greater than a threshold value ($0.001\ \mathrm{m^3/s}$), the term $2\,g\,H_u/\left(u_2^2\,\eta_p\right)$ is a linear function of $Q$, Figure 7.

In the linearity range, the coefficients of the previous equation can be calculated by best fitting the pump data sheet discrete values, Figure 8, and therefore it is possible to estimate the unknown values of the mechanical efficiency $\eta_m$ and the volumetric efficiency $\eta_v$.

Specifically, the mechanical efficiency is equal to $\eta_m = 0.955$ and it is assumed constant for the whole operating regime, whereas the volumetric efficiency obtained from this procedure represents the asymptotic limit only in the range of high flow rates and it is equal to $\eta_{v\infty} = 0.719$.

Known the value of the mechanical efficiency, from the (22), $\eta_v$ can be made explicit as function of the flow rate only, such as $\eta_v = \eta_v(Q)$.

The relationship $\eta_v = \eta_v(Q)$ is well described by the following relation:

$$\eta_v = \eta_{v\infty}\left(1-\mathrm{e}^{-\frac{Q}{\tau}}\right), \tag{23}$$

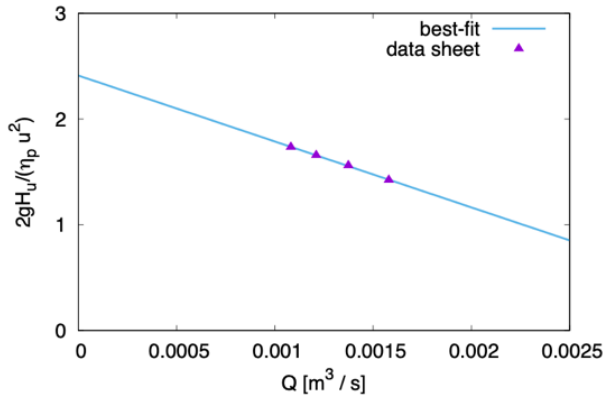


Figure 8. Linear regression of experimental data for the left-hand side term of (22) as function of the flow rate.

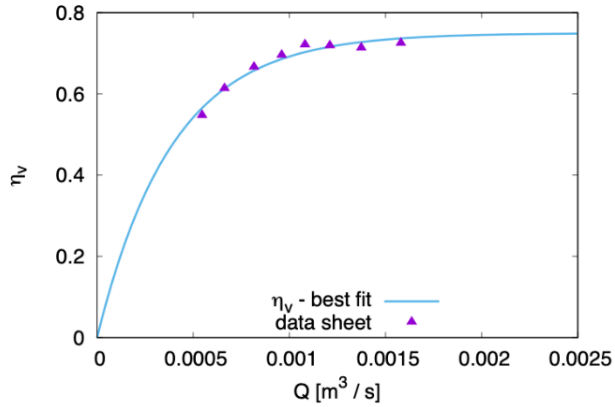


Figure 9. Least square regression of $\eta_v$ experimental data.

where the value of $\tau = 3.83 \cdot 10^{-4} m^3/s$ is obtained from the best-fit polynomial of the available data operation data of the pump with $\eta_{v\infty} = 0.719$. The following figure shows the good agreement between the theoretical prediction and pump data over the whole range of the flow rates.

The simulator function uses this model of the volumetric efficiency and the prediction of the mechanical efficiency. It provides a good agreement of the control parameters with the characteristic data of the pump, in terms of absorbed power $P_a$, efficiency $\eta_p$ and pressure head $H_u$.

Through the simulator, described in the previous section, it is possible to digitally reconstruct the pump characteristic curves, Figure 10, Figure 11 and Figure 12.

By using the digitalized technical and operating data of the system components and setting a value of the frequency of the inverter regulating the number of revolutions of the pump-motor block, this one can be iteratively determined from (19), and then the outputs of the pump-motor are calculated from its model, i.e. the flow rate, the head, the torque $C_m$ and the efficiency of the pump $\eta_p$, which constitute the virtual values with which to compare the physical ones acquired (and calculated, such as mechanical and volumetric efficiencies) by the sensors prepared for that purpose in the system.

So, the entire performance curves of the pump can be reconstructed and digitalized just varying the opening degree of the valve for each of the desired discrete values of the frequency (revolution speed of the pump), and by reiterating the use of the simulator equations as reported in the sections.

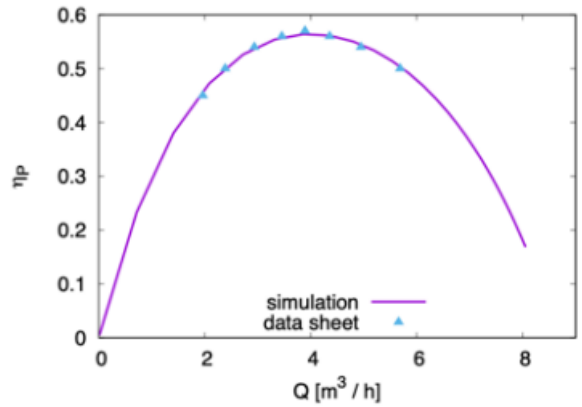


Figure 10.Expected pump efficiency from the simulator compared with actual operational points.

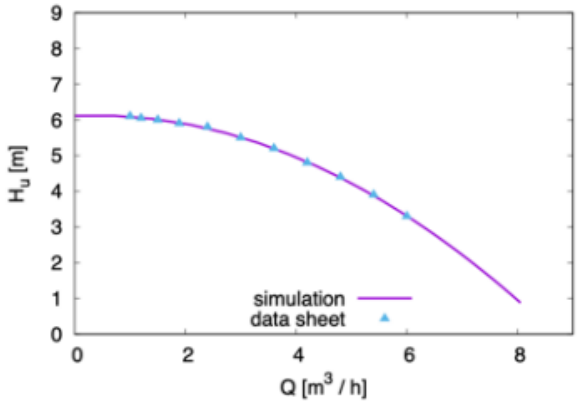


Figure 11. Expected pump manometric head from the simulator compared with actual operational points.

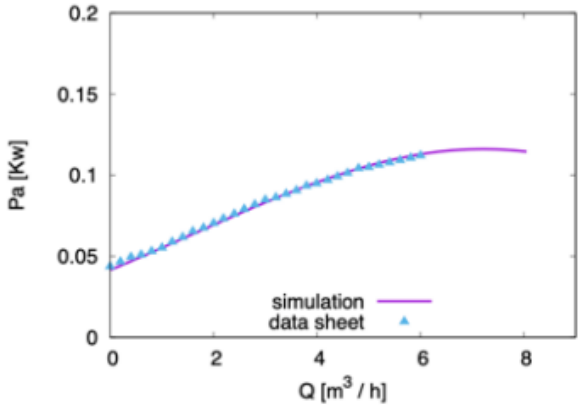


Figure 12. Expected pump absorbed power from the simulator compared with actual operational points.

The Figure 13 shows the pump performance curves evaluated by the simulator for 3 revolution speed values, as example of its application.

The operating parameter values predicted by the models, including the mechanical and volumetric efficiency, are the reference targets for eventual anomalies detection when compared with the relative acquired values. The eventual significative discrepancy between the predicted and sensed values of each characteristic quantity can indicate an incipient criticality for the component whom it refers to.

In these conditions it is possible to report and provide for the irregularity of the operation with an active control on the system. In addition, it is even possible to understand the origin of the disagreement between the real and expected values of mechanical or volumetric efficiency. For example, with reference to their possible discrepancy it is possible to suspect a critical condition of the bearings or seals of the pump-motor block.

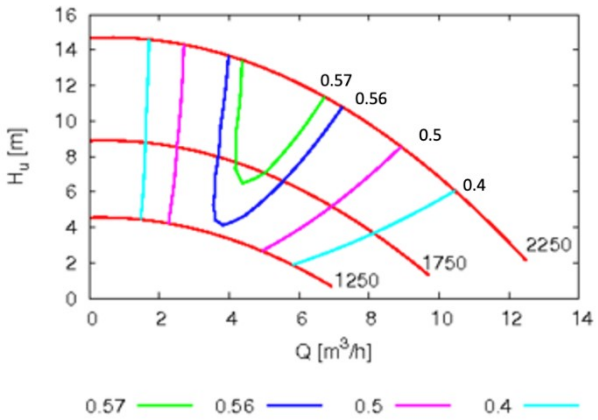


Figure 13. Expected pump performance curves from the simulator for three revolution speed (red lines) and four $\eta_p$ iso-lines.

## 5. DISCUSSION AND CONCLUSION

The intent of the authors was to propose a strategy for the automation of the monitoring of wide-ranging industrial processes, in the spirit of the "Smart Industry", in order to reduce the risks of sudden default of the activities caused by the possible criticality of the most delicate components, to reduce the time to identify the criticality, to reduce the maintenance time necessary to restore normal operating conditions, thus reducing the associated costs. The strategy is based on the creation of a virtual simulator of the operation of the various plants involved in the process which, through the digitization of the data sheets of the various components, can provide the reference values of the process control parameters. Those values are so compared with the values acquired by the measuring chains predisposed for the purpose, to allow the operator the reporting of any suspected anomaly in place and to quickly intervene to restore optimal operating conditions through targeted maintenance. To this end and by way of an example, we have proposed the formulation of a simulator of a simple fluidic thrust system, consisting of a pump-motor block with inverter and a regulation valve, which represents the load acting on the PM block and attributable to the network it supplies. The simulator allows to manage and analyze in real time all the characteristic parameters, acquired and/or calculated, of each of the monitored system components, during normal operation, to determine if there are conditions of possible incipient anomalies on the components under observation. This operation allows to compare, through real-time acquisitions, the instantaneous values of the characteristic operating parameters with those provided by the simulator, corresponding to those that should be in the optimal operating conditions of the system. So, it is possible to identify which characteristic parameter of the various monitored components of the system reveals a more discrepant value from the optimal one, thus denouncing a possible critical condition of the component to which it refers to. In this way, the operator can decide to intervene on the component in time, thus minimizing the intervention times and therefore the maintenance and restoration costs of the normal operation of the system. Is opinion of the authors that the identified procedure, based on the digitization of the technical data sheets of the plant components, is extendable to most of the operating plants of an industrial process, thus allowing the entire process to be controlled in real time.

## REFERENCES

[1] R. A. Luchian, G. Stamatescu, I. Stamatescu, I. Fagarasan, D. Popescu, IIoT Decentralized System Monitoring for Smart Industry Applications, 2021 29th Mediterranean Conference on Control and Automation (MED), 2021, pp. 1161-1166. DOI 10.1109/MED51440.2021.9480341

[2] L. Fabbiano, G. Vacca, G. Dinardo, Smart water grid: A smart methodology to detect leaks in water distribution networks,

Measurement, Vol. 151, (2020).
DOI: 10.1016/j.measurement.2019.107260

[3] L. Ardito, A. Messeni Petruzzelli, U. Panniello, A. Garavelli, Towards Industry 4.0: Mapping digital technologies for supply chain management-marketing integration, Business Process Management Journal, Vol. 25, (2019), No. 2, pp. 323-346. DOI: 10.1108/BPMJ-04-2017-0088

[4] A. J. Isaksson, I. Harjunkoski, G. Sand, The impact of digitalization on the future of control and operations, Comput. and Chem. Eng., 114, (2018), pp. 122–129. DOI: 10.1016/j.compchemeng.2017.10.037

[5] G. Dinardo, L. Fabbiano, G. Vacca, A smart and intuitive machine condition monitoring in the Industry 4.0 scenario. Measurement, 126, (2018), pp. 1–12. DOI: 10.1016/j.measurement.2018.05.041

[6] M. Short, J. Twiddle, An Industrial Digitalization Platform for Condition Monitoring and Predictive Maintenance of Pumping Equipment. Sensors, 19, (2019), 3781. DOI: 10.3390/s19173781

[7] P. Girdhar, C. Scheffer, Predictive maintenance techniques: Part 1 predictive maintenance basics, in Practical Machinery Vibration Analysis and Predictive Maintenance, P. Girdhar and C. Scheffer, Eds., Oxford, Newnes, (2004), pp. 1-10.

[8] P. Girdhar and C. Scheffer, Predictive maintenance techniques: Part 2 vibration basics, in Practical Machinery Vibration Analysis and Predictive Maintenance, P. Girdhar and C. Scheffer, Eds., Oxford, Newnes, (2004), pp. 11-28.

[9] M. Caciotta, V. Cerqua, F. Leccese, S. Giarnetti, E. De Francesco, E. De Francesco, N. Scaldarella, A first study on prognostic system for electric engines based on Envelope Analysis, In IEEE Metrology for Aerospace (2014), Benevento, Italy, 29-30 May 2014, pp. 362-366. DOI: 10.1109/MetroAeroSpace.2014.6865950

[10] T. Van Tung, Y. Bo-Suk, Machine fault diagnosis and prognosis: The state of the art, International Journal of Fluid Machinery and Systems 2.1, (2009), pp. 61-71. DOI: 10.5293/IJFMS.2009.2.1.061

[11] Li Zhe, Yi Wang, Ke-Sheng Wang, Intelligent predictive maintenance for fault diagnosis and prognosis in machine centers: Industry 4.0 scenario, Advances in Manufacturing 5.4, (2017), pp. 377-387. DOI: 10.1007/s40436-017-0203-8

[12] E. Petritoli, F. Leccese, G. Schirripa Spagnolo, New reliability for industry 4.0: A caste study in COTS-based equipment, IEEE International Workshop on Metrology for Industry 4.0 & IoT (MetroInd4.0&IoT), Rome, Italy, 7-9 June 2021, pp. 27-31. DOI: 10.1109/MetroInd4.0IoT51437.2021.9488555

[13] E. Quatrini, F. Costantino, G. Di Gravio, R. Patriarca, Condition-Based Maintenance - An Extensive Literature Review, Machines, (2020), 8, 31, pp. 1-28. DOI: 10.3390/machines8020031

[14] A. K. S. Jardine, D. Lin, D. Banjevic, A review on machinery diagnostics and prognostics implementing condition-based maintenance, Mechanical Systems and Signal Processing, vol. 20, (2006), pp. 1483-1510. DOI: 10.1016/j.ymssp.2005.09.012

[15] Caldepa website. Online [Accessed 03 November 2021] https://pump-selector.calpeda.com/pump/23

[16] F. Fornarelli, A. Lippolis, P. Oresta, A. Posa, Computational Investigation of a pressure compensated vane pump, Energy Procedia, Volume 148, 73rd Conference of the Italian Thermal Machines Engineering Association, Pisa, Italy, 12 September 2018, pp 194-201. DOI: 10.1016/j.egypro.2018.08.068